Supplementary Figures

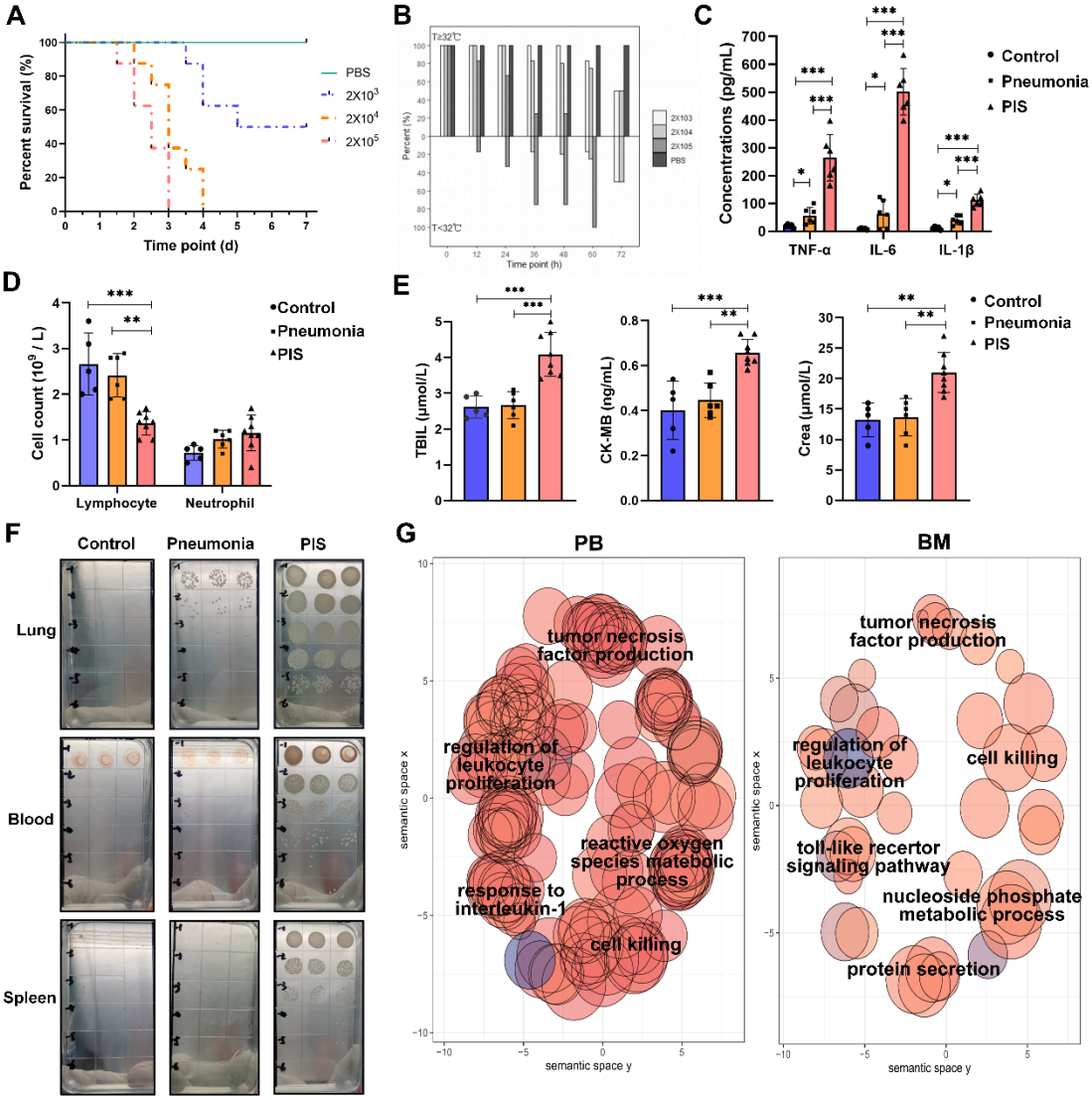

Supplementary Figure 1. Supplementary data of *K.p*-induced sepsis model and bulk-RNA sequence. Inoculation with PBS (control) and *K.p* (2×10^3, 2×10^4, and 2×10^5 CFU), **(A)** the survival rate (n = 10 mice/group) and **(B)** low temperature (< 32 ℃) percent in each group. **(C)** Quantitative bar charts showing concentrations of TNF-α, IL-6, and IL-1β concentrations in BALF samples. **(D)** Quantitative bar charts showing lymphocyte and neutrophil counts in peripheral blood. **(E)** Comparisons of blood biochemical indexes indicating liver (TBIL), heart (CK-MB), and kidney (Crea) functions, as calculated by ANOVA. **(F)** Representative diaphragms of viable bacteria recovered from lung, blood, and spleen in control, pneumonia, and PIS groups. **(G)** Based on DEGs from PB and BM, the visualization of representative GO terms after eliminating redundancy with Revigo. Statistical significances were calculated using the Brown-Forsythe and Welch analysis of variance (ANOVA) test unless otherwise indicated. Data were presented as mean ± SD. *$p < 0.05$, **$p < 0.01$, ***$p < 0$ .001.

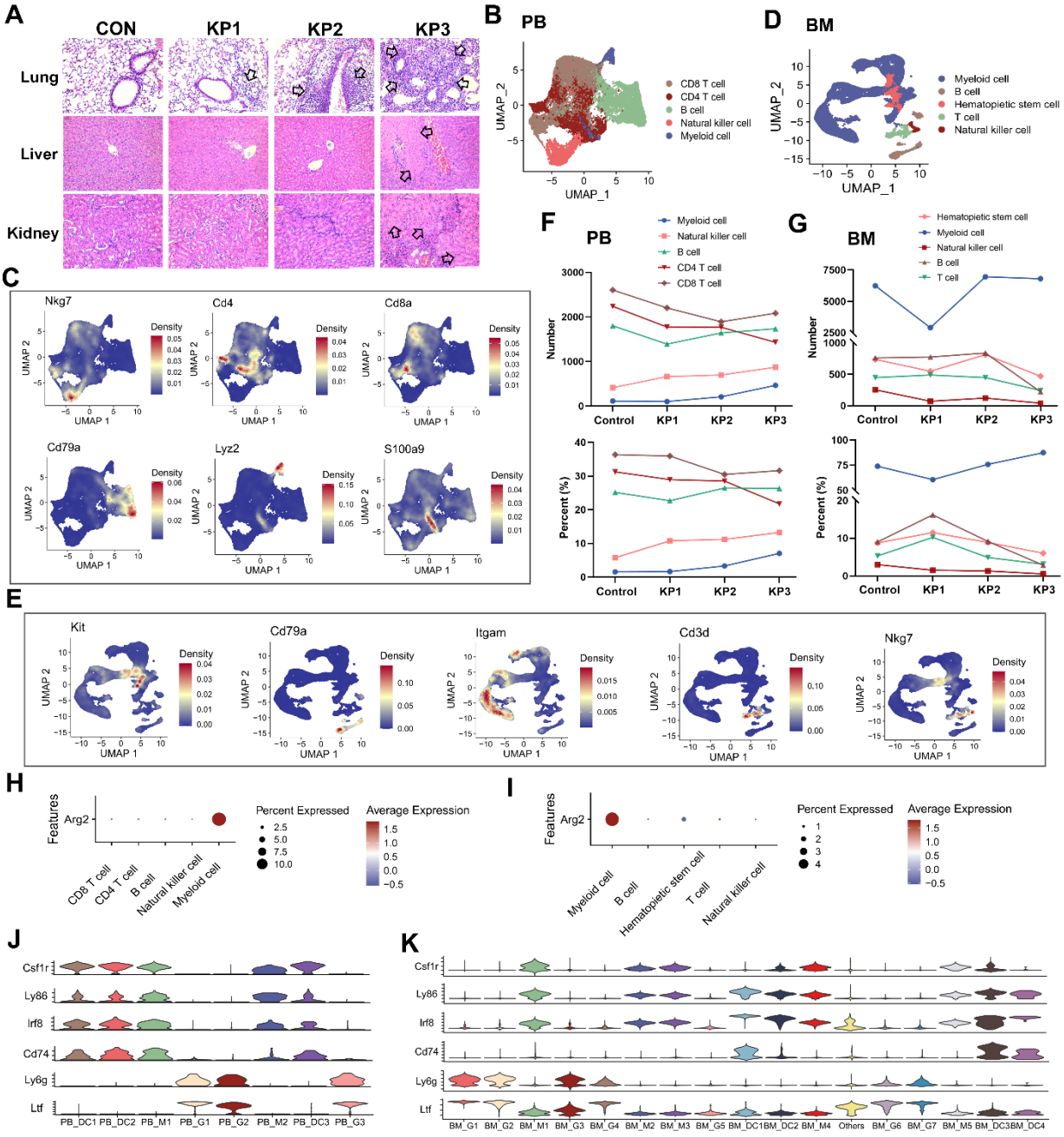

Supplementary Figure 2. Supplementary data of sc-RNA seq analysis. (A) Representative HE results of lung, liver, and kidney tissues from the PIS model at CON, KP1, KP2, and KP3 four stages. Black arrows indicated pathological areas. **(B)** After quality control, the two-dimensional UMAP distribution for 26,088 sequenced PBMCs was divided into five main types of immune cells. **(C)** Classical genes for cell-type identification in PBMC, *Nkg7* for natural killer cells, *Cd4* for CD4 T cells, *CD8a* for CD8 T cells, *Cd79a* for B cells, and *Lyz2* and *S100a9* for myeloid cells. **(D)** The two-dimensional UMAP distribution for 30,171 sequenced BM cells after quality control, which were divided into five main cell types. **(E)** Classical genes for cell-type identification in BM cells, while *Kit* for hematopoietic stem cells, *Cd79a* for B cells, *Cd3d* for T cells, *Nkg7* for natural killer cells, and *Itgam* for myeloid cells. **(F and G)** The number and proportion of main cell types in **F** PB and **G** BM with PIS progression.

(H and I) The dotplot exhibited the dominant *Arg2* expression in myeloid cells rather than other cell types in **H** PB and **I** BM samples. **(J and K)** The violin plot displayed the expression levels of classical genes in **J** PB- and **K** BM-derived myeloid clusters, while the *Irf8* and *Cd74* for dendritic clusters, the *Csf1r* and *Ly86* for monocyte clusters, and the *Ltf* as well as *Ly6g* for granulocyte clusters.

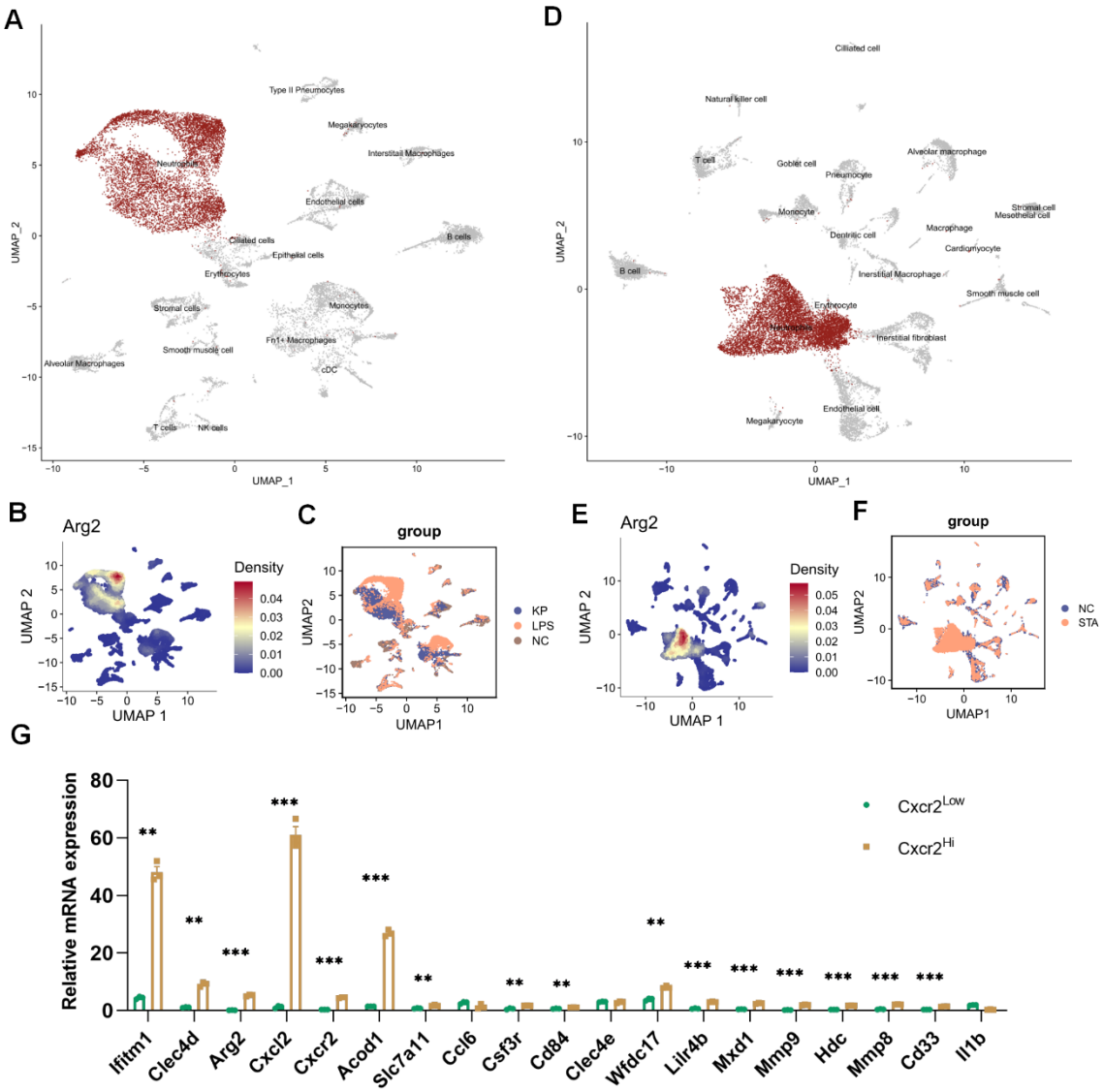

Supplementary Figure 3. ***Arg2*** **was enriched in granulocyte subsets in lung tissue from LPS- and bacteria-stimulated mice. (A-C)** The **A** two-dimensional UMAP distribution of lung samples from **B** *K.p* or LPS intratracheally inoculated and control (NC) mice in public sc-RNA dataset GSE190262, while the **C** *Arg2* transcript was primarily expressed in neutrophils. **(D-F)** The **D** two-dimensional UMAP distribution of lung samples from **E** staphylococcus aureus intratracheally inoculated and control (NC) mice in public sc-RNA dataset GSE215195, while the **F** *Arg2* transcript was primarily expressed in neutrophils. **(G)** RT-PCR assay showing the high expression of selected signature genes of ARG2 enriched MDSCs in the CXCR2^{Hi} subset from KP mice. Statistical significances were calculated by unpaired t-test. Data were presented as mean ± SD. $^{**}p < 0.01$, $^{***}p < 0.001$.

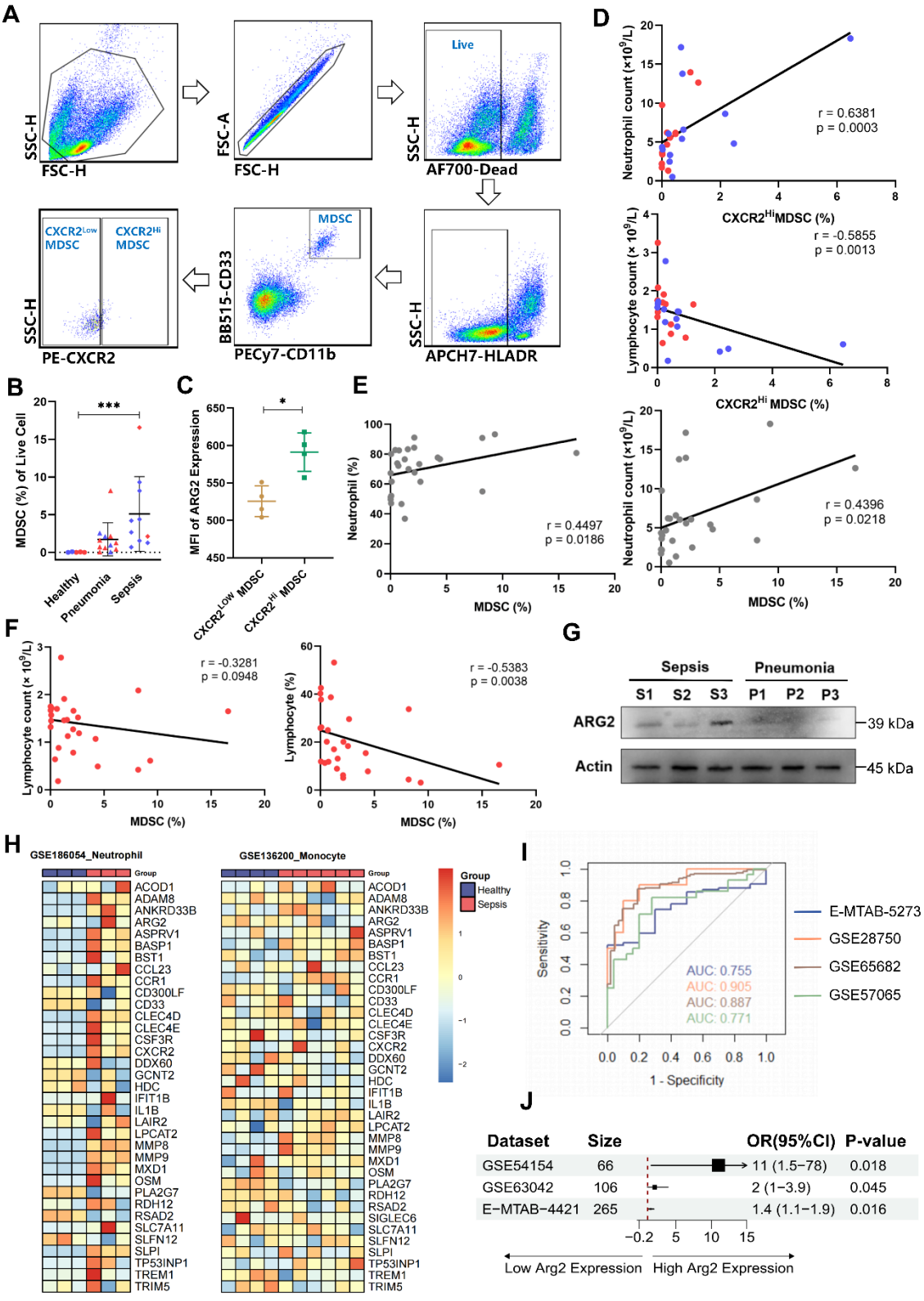

Supplementary Figure 4. The ARG2 enriched CXCR2^{Hi} MDSCs associated with low lymphocyte counts and poor prognosis in clinical scenarios and suppressed the proliferation of CD4+ T cells through its type II arginase role *in vitro*. (A) Gating strategy of HLA-DR^{Low}CD11b^{+}CD33^{+} MDSCs and HLA-DR^{Low}CD11b^{+}CD33^{+}CXCR2^{Hi} MDSCs in white blood cells from clinical patients, as

detected by flow cytometry. **(B)** Statistics of proportions of total MDSCs between healthy volunteers (n = 5), pneumonia patients (n = 12), and septic patients (n = 10), as calculated by the Mann-Whitney test. Red and blue dots represented female and male individuals, respectively. **(C)** The flow cytometry detected the higher ARG2 expression in $CXCR2^{Hi}$ MDSCs than in the $CXCR2^{Low}$ subset. **(D)** A significant positive correlation between the percentage of $CXCR2^{Hi}$ MDSCs and neutrophil counts and a negative correlation between the percentage of $CXCR2^{Hi}$ MDSCs and lymphocyte counts. Red and blue dots represented female and male individuals, respectively. **(E)** Correlations between the percentage of MDSCs and neutrophil count and neutrophil proportion. **(F)** Correlations between the percentage of MDSCs and lymphocyte count and lymphocyte proportion. **(G)** Protein levels of ARG2 were higher in blood samples from the PIS than the pneumonia (n = 3 patients/group). **(H)** Signature genes of $CXCR2^{Hi}$ MDSC expressed highly in neutrophils (GSE186054) rather than in monocytes (GSE136200) from septic patients. **(I)** The receiver operator curves (ROC) for applying *Arg2* expression in sepsis diagnosis in four bulk transcriptome datasets, with all areas under curve (AUCs) more than 0.75. **(J)** The high *Arg2* expression were associated with 28-day death events in three datasets. Odds ratio (OR) was calculated by Logistic univariate regression. Data were presented as mean ± SD. ***$p < 0.001$.

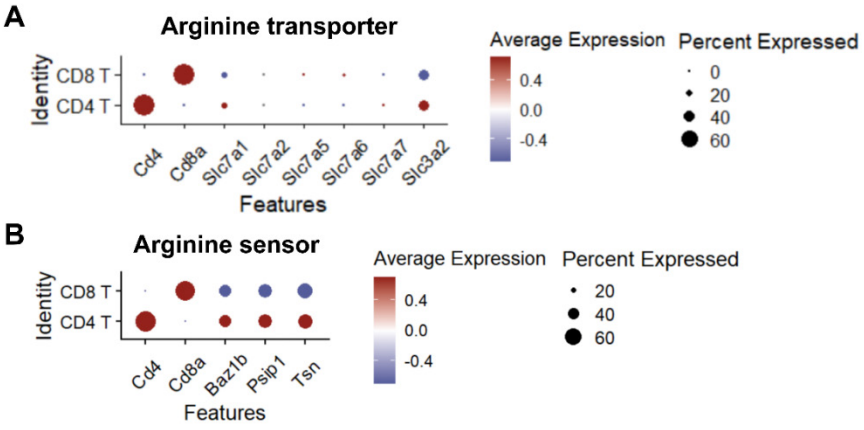

Supplementary Figure 5. (A and B) The dot plot showing differences in expression levels of **A** arginine transporters and **B** arginine sensors in splenic $CD4^+$ and $CD8^+$ T cells.

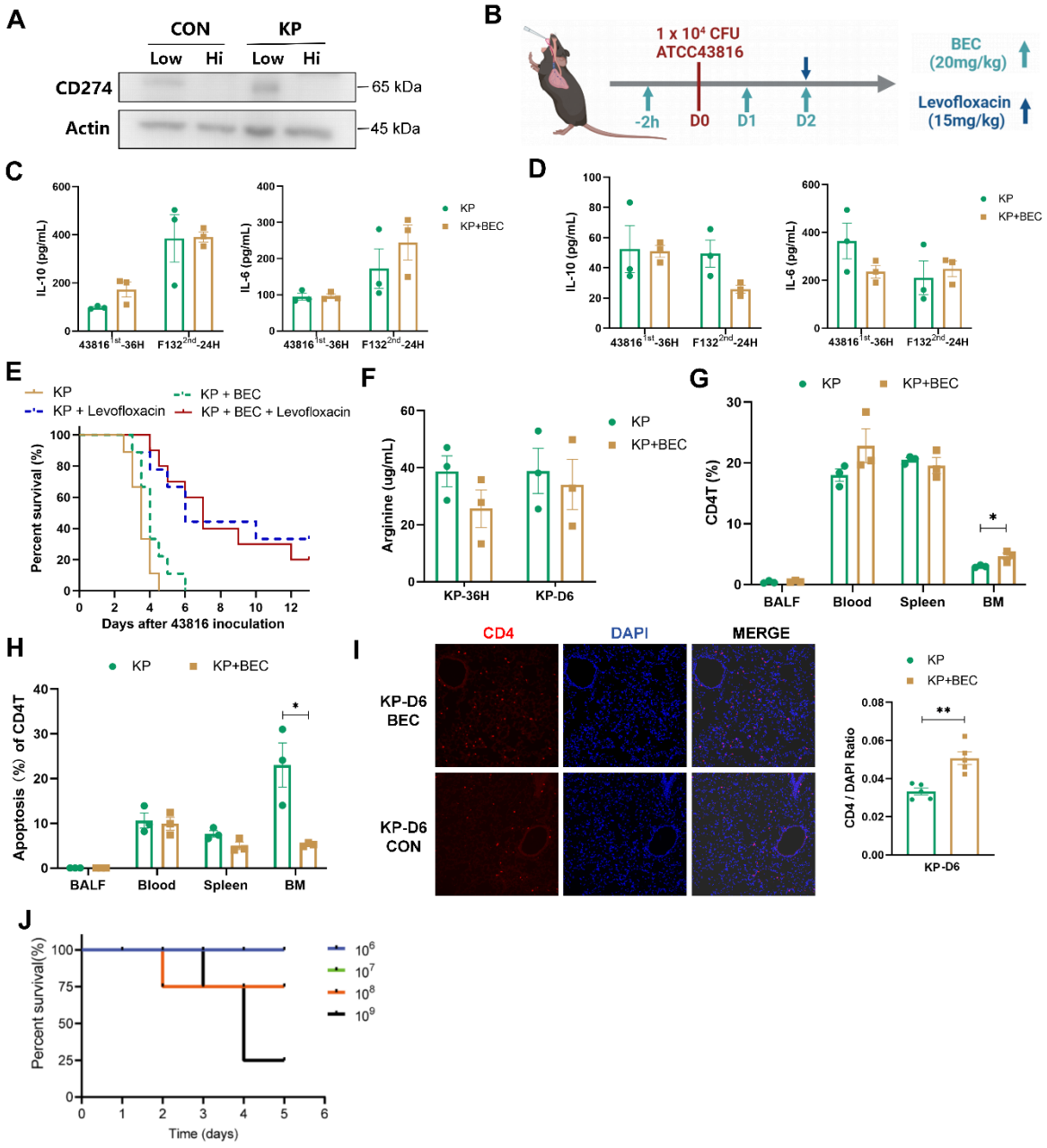

Supplementary Figure 6. ARG2 inhibitor BEC did not impact inflammatory responses and outcomes in first infection. (A) Protein expression level of immune checkpoint CD274 (PDL1) in $CXCR2^{Low}$ MDSC and $CXCR2^{Hi}$ MDSC by western blotting. **(B)** Schematic diagram of the treatment and sample collection procedures for PIS animal experiments, with infection of *K.p* stain #ATCC43816. **(C and D)** Concentrations of IL-10 and IL-6 in **C** BALF and **D** plasma samples at 36 hours after first infection and at 24 h after secondary infection. Patients. n = 3 biologically independent mice. **(E)** Kaplan-Meier survival curve of four mice groups (n = 8 mice/group) including KP, KP with BEC administration, and both with levofloxacin treatment or not. **(F)** The arginine concentration in plasma at 36 h and Day 6. n = 3 biologically independent mice. **(G and H)** Statistics on the **G** $CD4^+$ T cell percentage and its **H** apoptotic rates in BALF, BM, spleen, and blood at 36 h after *K.p* inoculation. Statistical significance is calculated by unpaired t-test. n = 3 biologically independent

mice. **(I)** Representative results (left) and statistics (right) of the immunofluorescence of lung tissue at Day 6 after *K.p* inoculation. Red indicated CD4, and blue indicated DAPI. **(J)** The survival rate of mice inoculating with F132 (1×10^6, 1×10^7, 1×10^8 and 1×10^9 CFU) (n = 6 mice/group). Statistical significances were calculated by unpaired t-test. Data are presented as mean ± SD. * $p < 0.05$, ** $p < 0.01$.

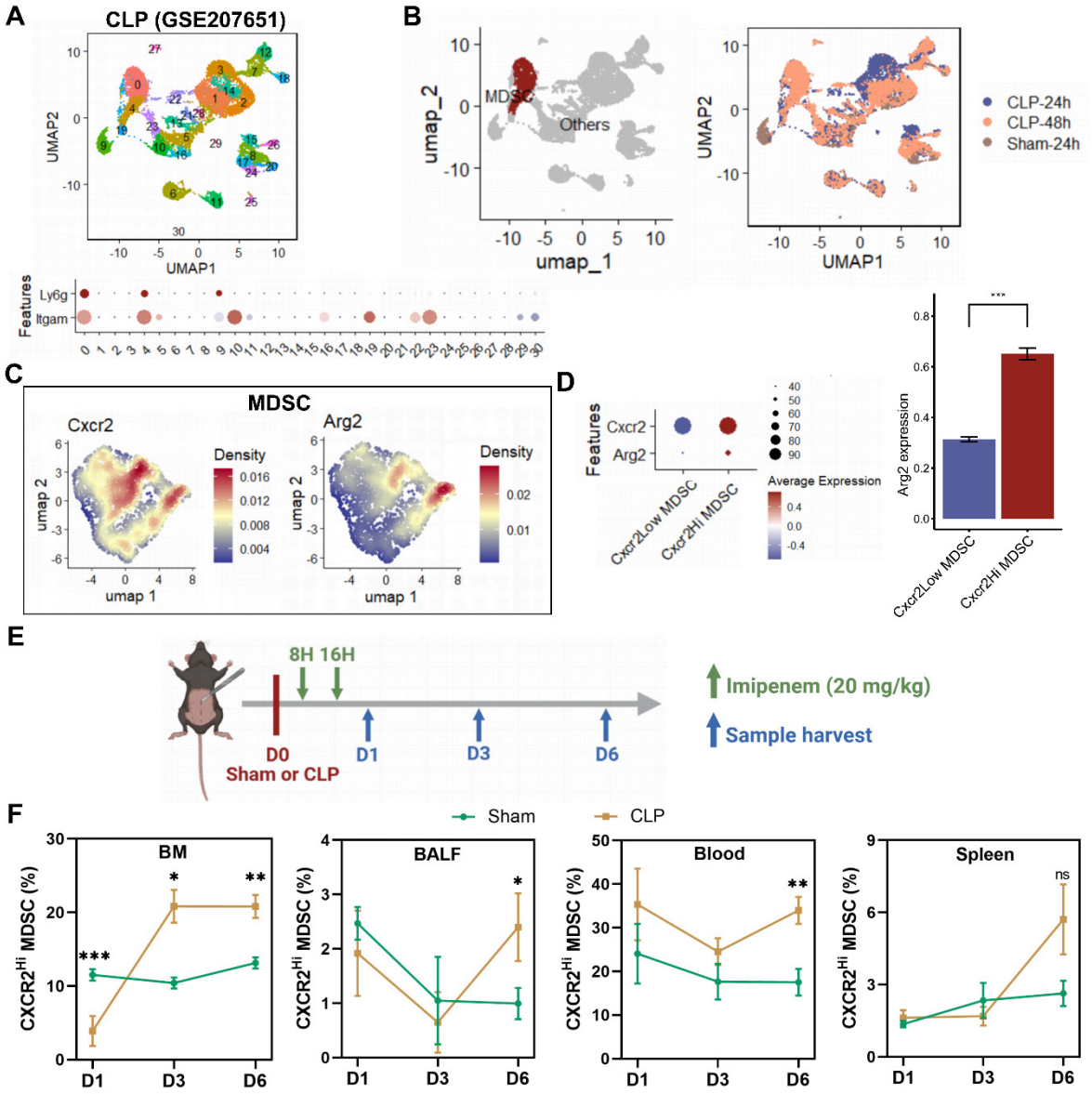

Supplementary Figure 7. The ARG2-enriched CXCR2^{Hi} MDSCs increased at a later stage in another septic model of cecum ligation and puncture (CLP). **(A)** The two-dimensional UMAP distribution of lung samples from CLP mice in public sc-RNA dataset GSE207651, while the cluster 0 and cluster 4 highly expressed MDSCs' marker genes *Ly6g* and *Cd11b*. **(B)** The MDSCs (cluster 0 and cluster 4) increased in the CLP rather than the Sham. **(C)** The expression and distribution of *Cxcr2* and *Arg2* transcripts in MDSCs. **(D)** Similar to the PIS model, in the CLP model, the *Arg2* transcript was significantly enriched in the MDSC subset with high *Cxcr2* expression. The statistical significance was analyzed using the Wilcoxon test. **(E)** Schematic diagram of the antibiotic treatment and sample collection procedures for CLP animal experiments. **(F)** The dynamic detection of CXCR2^{Hi} MDSCs in BM, BALF, blood, and spleen showed their accumulation at D6 after surgery. n = 3-4 biologically independent mice. Statistical significances were calculated by the unpaired t-test. *$p < 0.05$, **$p < 0.01$, ***$p < 0.001$.

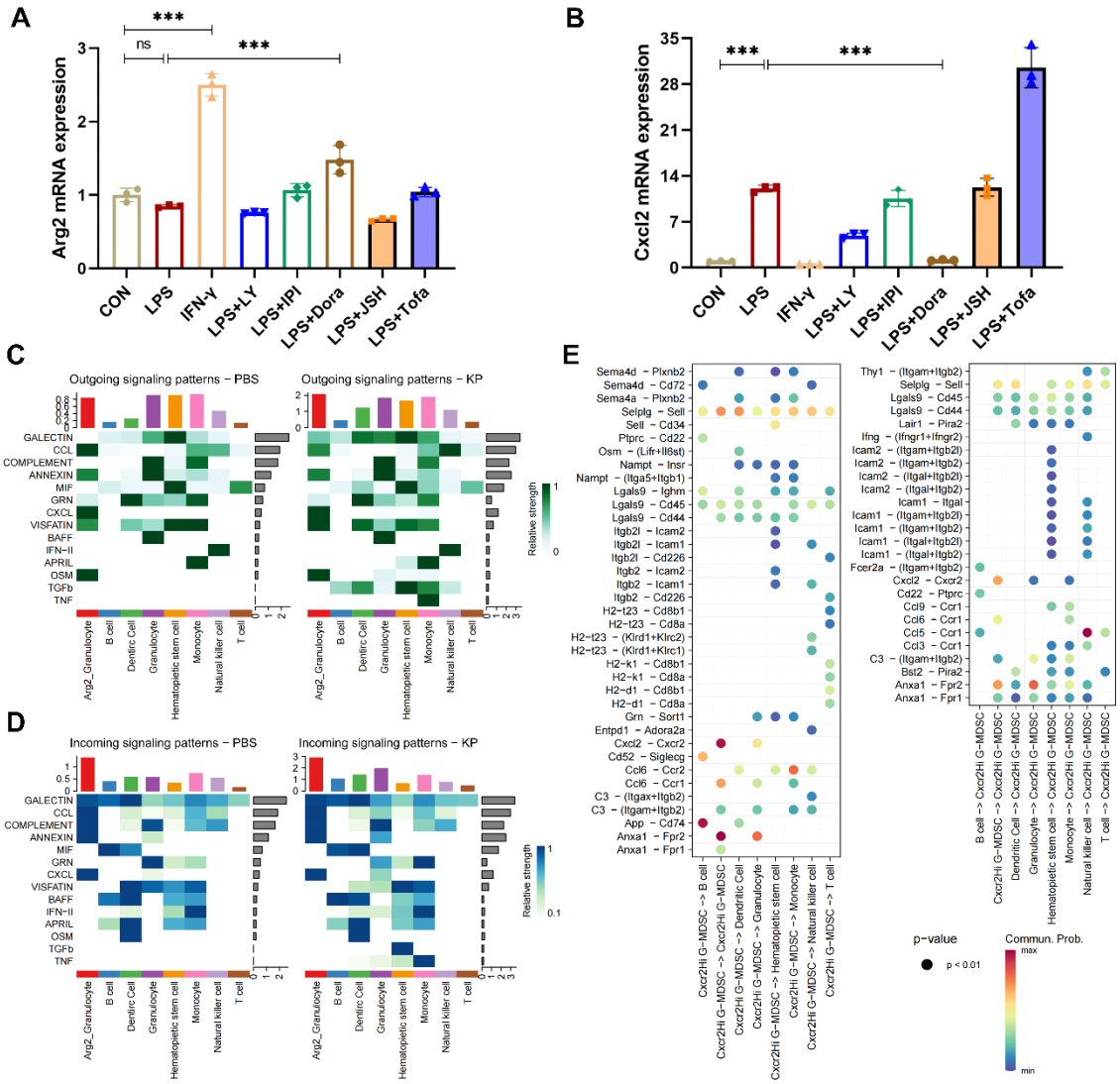

Supplementary Figure 8. The cell-cell communication analysis predicted substantial Cxcl2-Cxcr2 crosstalk between ARG2-enriched CXCR2^{Hi} MDSCs and itself. (A and B) The mRNA expression levels of **A** *Arg2* and **B** *Cxcl2* in CXCR2^{Hi} MDSCs after treatment with LPS, IFN-γ, and pathway inhibitors. LY: The PI3Kα, PI3Kδ, and PI3Kβ inhibitor LY294002. IPI: The PI3Kγ inhibitor IPI594. Dora: The p38-MAPK inhibitor Doramapimod. JSH: The NF-κB inhibitor JSH-23. Tofa: The JAK inhibitor Tofacitinib. Data were represented as mean ± SD.**(C and D)** The heatmap showed overall **C** incoming and **D** outgoing signaling of cell-cell communications in all cell types at CON (PBS) and KP stages. **(E)** The dot plot showed cell-cell communication probabilities between CXCR2^{Hi} MDSCs as the sender (left) or target (right) and other cell types, including B cells, dendritic cells, granulocytes, hematopoietic stem cells, monocytes, natural killer cells, and T cells.

Supplementary Tables

Supplementary Table 1. The assessment items and judging standards of pneumonia-induced sepsis (PIS) mice.

Assessment items	Manifestations of the pneumonia-induced sepsis
Temperature	< 32℃
Behaviors	
Fur aspect	Piloerection, tarnished
Posture	Hunched and curled up
Breath state	Severely dyspnea with thoracic abdominal respiration
Activity	No relocation when stimulated†
Eye lids	Closed in usual, slightly open when stimulated*

*: Stimulated state: Lid off the box and gently touched mice. Mice met all above criteria were identified as the PIS mouse.

Supplementary Table 2. The body temperature in survived mice inoculation with PBS (control) and *K.p* (2×10^3, 2×10^4, and 2×10^5 CFU).

		Survived mice (n)	1	2	3	4	5	6	7	8	9	10
0h	PBS	10	37.2	37.4	37.9	37.4	37.6	37.9	37.3	37.9	38	37.6
	2×10^3	10	37.9	37	38.2	37.9	37.4	37.7	37.6	37.4	38	37.2
	2×10^4	10	36.9	38.2	37.0	37.1	37.9	37.3	37.2	38.1	37.8	37.5
	2×10^5	10	37.5	37.3	37.6	38	37.1	37.9	37.1	38	37.5	37.9
12h	PBS	10	37.3	37.8	38	37.3	37.5	37.4	38.1	37.6	37.1	37.6
	2×10^3	10	37.1	37.7	38	36.7	38	37.8	37.6	37.2	37.2	36.9
	2×10^4	10	37	36.8	37.1	37.8	37.4	37	36.4	37.2	36.6	36.1
	2×10^5	10	< 32	< 32	35.2	36	35.4	35.6	35.2	34.8	34.9	35.1

24h	PBS	10	38.1	37.1	36.9	37.5	37.6	37.8	37.8	36.9	37.3	37.5
	2×10^3	10	37.2	38	36.4	37.2	37.3	37.3	37.6	37.2	36.9	37.1
	2×10^4	10	36.3	35.9	36.7	36.8	35.1	37	35.9	36.3	36	35.8
	2×10^5	10	< 32	< 32	< 32	33.3	34.2	34.9	35.8	32.5	33.4	33.1
36h	PBS	10	36.6	36.9	38.2	38	37.8	36.8	37.6	37.1	37.9	38
	2×10^3	10	37.3	36.9	37.1	37.3	36.5	37	35.9	36.4	37.5	36.9
	2×10^4	10	< 32	< 32	34	34.7	33.6	35.5	35.8	36	35.2	33.4
	2×10^5	9	< 32	< 32	< 32	< 32	< 32	< 32	< 32	33.5	32.9	
48h	PBS	10	37.6	38.0	37.2	37.0	37.6	37.9	37.7	37.3	37.7	38.1
	2×10^3	10	37	36.7	37.1	36.4	36.5	37.8	36.6	35.4	36.5	34.9
	2×10^4	9	< 32	< 32	35.8	34	35.2	35.7	33.4	36.2	32.3	
	2×10^5	6	< 32	< 32	< 32	< 32	< 32	32.4				
60h	PBS	10	37.9	37.4	37	37.5	36.8	37.9	37.3	38.1	37.9	37.4
	2×10^3	10	< 32	< 32	35.6	33.5	37	36.4	34.7	37.2	33.9	32.9
	2×10^4	7	< 32	< 32	33	34.6	33.8	35.1	34.2			
	2×10^5	4	< 32	< 32	< 32	< 32						
72h	PBS	10	37.3	37	37.1	37.4	38.1	37.6	37.6	36.9	37.4	37.2
	2×10^3	10	< 32	< 32	< 32	< 32	< 32	35.3	36.9	35.8	36.5	35.7
	2×10^4	4	< 32	< 32	32.2	32.6						
	2×10^5	0										

Supplementary Table 3. Characteristics of public transcriptomic datasets included in this study.

Dataset	Download platform	Specie	Experiment type	Sample
GSE190262	GEO	mouse	scRNA-seq	Lung (*K.p* infected and LPS administrated)
GSE215195	GEO	mouse	scRNA-seq	Lung (STA infected)
GSE207651	GEO	mouse	scRNA-seq	Lung (Sham and CLP)
GSE222784	GEO	mouse	scRNA-seq	Spleen (healthy)
GSE186054	GEO	human	RNA-Seq	Neutrophil (sepsis)
GSE136200	GEO	human	RNA-Seq	Monocyte (sepsis)
E-MTAB-5273	ArrayExpress	human	Array	Whole-blood leukocyte (sepsis)
GSE28750	GEO	human	Array	Whole-blood leukocyte (sepsis)
GSE65682	GEO	human	Array	Whole-blood leukocyte (sepsis)
GSE57065	GEO	human	Array	Whole-blood leukocyte (sepsis)
GSE54154	GEO	human	Array	Whole-blood leukocyte (sepsis)
GSE63042	GEO	human	RNA-Seq	Whole-blood leukocyte (sepsis)
E-MTAB-4421	ArrayExpress	human	Array	Whole-blood leukocyte (sepsis)

Supplementary Table 4. Gene lists for functional scoring of ARG2 enriched CXCR2^{Hi} MDSCs.

MDSC	Specific_granules	NADPH_oxidase	Azurophil_granulesb
Wfdc17	Lyz2	Cybb	Hexa
Ifitm1	Lcn2	Cyba	Prss57
Il1b	Cyba	Rac2	Prtn3
BC100530	Cybb	Rac1	Ctsg
Srgn	Ncf1	Ncf2	Elane
Gm5483	Ncf4	Ncf1	Mpo
Stfa2l1	Ltf	Ncf4	Ctsc
Stfa2	Camp		
Prok2			
Ifitm2			
Junb			
Dusp1			
Socs3			
Btg1			
1600014C10Rik			
Selplg			
Asprv1			
Igfbp6			
Gm5150			
Pla2g7			

Csf3r
Cxcr2
Tpd52
Tspo
Cyp4f18
Grina
Fabp5
Clec4d
Steap4
Map1lc3b
Ccr1
Lrg1
Clec4e
Ctsd
Cd84
Gcnt2
Arg2
BC117090
Npl
Fgl2
Rnf149
Sephs2
S100a6
Lmnb1
Amica1
Eif4ebp1
Msrb1
Ubb
C5ar1
Ypel3
Fcgr3
Gsr
Taldo1
Atp6v1g1
S100a11
Hp
Alox5ap
Litaf
Txn1
Upp1
AB124611
Gpcpd1
Snap23
Il4ra

Hist1h2bc
Retnlg
Myd88
Adipor1
Stk17b
Zyx
Rgs3
Il1f9
Hdc
Atg3
Gda
Slc40a1
Tarm1
Cdk2ap2
Stfa3
Glipr2
Tacstd2
Picalm
Mtus1
Fbxl5
Slfn1
Rnd1
Ier2
Mxd1
Siglece
Cdkn2d
Cd33
Lilr4b
Cd14
Sell
Ppt1
Skap2
Sfxn5
2810474O19Rik
Ikbkap
Hbb-bs
Atp11b
Cxcl2
Osm
Ier3
Hba-a1

Supplementary Table 5. Signature genes of ARG2 enriched CXCR2^{Hi} MDSCs, as generated by COSG and Findmarker.

Gene	COSG score	Findmarker avg_log2FC	Findmarker p_val_adj
Acod1	0.482509878	0.883351576	0
Adam19	0.311860106	0.701278309	0
Adam8	0.26961558	0.775699974	0
Ankrd33b	0.433460111	0.641799542	2.57E-214
Asprv1	0.254473467	0.573986622	7.66E-140
Basp1	0.2201211	0.526687165	2.61E-284
Bst1	0.256930602	0.793884771	0
Ccl6	0.214639173	0.945517684	0
Ccr1	0.228939268	0.808657155	0
Cd300ld	0.392502449	0.766766799	0
Cd33	0.242934183	0.91289871	0
Clec4d	0.667115114	1.190757812	0
Clec4e	0.270275374	0.83313437	0
Csf3r	0.29936599	0.921790624	0
Cxcl2	0.511397525	1.396866626	0
Cxcr2	0.345942951	1.117188641	0
Ddx60	0.310148155	0.766520132	0
Dusp1	0.190028443	0.792135082	0
Gcnt2	0.249138911	0.612971562	3.22E-246
Hdc	0.27458751	1.007490567	0
Ifit1	0.2530592	0.543611083	7.69E-128
Ifitm1	0.437906303	1.036703285	0
Il1b	0.424069919	1.02966685	0
Il1rn	0.200209506	0.486095374	1.78E-268
Lilr4b	0.259126457	0.922138263	0
Lpcat2	0.196030948	0.57688202	3.35E-219
Mmp8	0.333321141	1.201330099	0
Mmp9	0.275491208	1.177669746	0
Mxd1	0.201604232	0.954805129	0
Oasl2	0.305812379	0.662344916	2.97E-234
Osm	0.283743976	0.779442319	0
Pla2g7	0.39287893	0.560911256	1.81E-172
Rdh12	0.230947726	0.636047995	8.08E-259
Retnlg	0.455043273	1.630525772	0
Rsad2	0.294173352	0.807244596	0
Slc7a11	0.414003548	1.145293412	0
Slfn1	0.205490753	0.687369064	0
Slpi	0.198002753	0.706446333	0
Timp2	0.228287072	0.502645359	1.28E-118

Trem1	0.2476877	0.735769243	0
Trim30b	0.384767346	0.818017842	0
Trp53inp1	0.254166001	0.648812225	3.57E-278
Wfdc17	0.316257379	0.794235914	1.84E-270

Supplementary Table 6. Demographics of clinical patients in this study.

Characteristics	Healthy (n = 5)	Pneumonia (n =12)	Sepsis (n = 10)	p value
Age, median (IQR)	54.00 (49.00, 60.00)	45.50 (28.50, 61.50)	68.50 (55.00, 72.00)	0.102
Sex, n (%)				0.091
Male	2 (40.0%)	4 (33.3%)	8 (80.0%)	
Medical history				
Hypertension, n (%)	2 (40.0%)	1 (8.33%)	3 (30.0%)	0.276
Diabetes, n (%)	1 (20.0%)	0 (0%)	3 (30.0%)	0.113
Chronic pulmonary disease, n (%)	4 (80.0%)	0 (0%)	6 (60.0%)	<0.001
Chronic cardiac disease, n (%)	1 (20.0%)	0 (0%)	6 (60.0%)	0.003
Chronic liver disease, n (%)	0 (0%)	1 (8.33%)	5 (50.0%)	0.041
Chronic kidney disease, n (%)	0 (0%)	1 (8.33%)	0 (0%)	>0.999
Solid malignant tumor, n (%)	1 (20.0%)	0 (0%)	3 (30.0%)	0.113
Laboratory findings				
Lymphocyte count ($\times 10^9$ /L), median (IQR)	1.72 (1.67, 1.75)	1.55 (1.24, 1.75)	0.93 (0.52, 1.39)	0.007
Neutrophil count ($\times 10^9$ /L), median (IQR)	3.60 (2.22, 4.04)	5.81 (3.39, 6.18)	7.61 (4.95, 13.50)	0.078
C-reactive protein (mg/L), median (IQR)	2.72 (0.50, 3.17)	4.91 (2.80, 24.09)	27.74 (9.65, 125.58)	0.068
Procalcitonin (mg/L), median (IQR)	NA	NA	14.31 (2.50, 98.50)	-
Outcomes				0.025
Survival, n (%)	5 (100%)	12 (100%)	6 (60%)	

Supplementary Table 7. Mouse-specie primers used in this study.

Gene	Forward	Reverse
Arg1	CTCCAAGCCAAAGTCCTTAGAG	AGGAGCTGTCATTAGGGACATC
Arg2	AGGAGTGGAATATGGTCCAGC	AGGGATCATCTTGTGGGACATT
CD84	ATATAGCTGGAGTCCCTTTGGAG	AAAGAGCACGGCCAATCCTC
Clec4d	CCTGCTGTCCTGTTAGCTGG	CTGTTCTGCTTCGGTGTTGAT
Wfdc17	TTTGATCACTGTGGGGATG	ACACTTTCTGGTGAAGGCTTG
Clec4e	AGTGCTCTCCTGGACGATAG	CCTGATGCCTCACTGTAGCAG
Cxcr2	ATGCCCTCTATTCTGCCAGAT	GTGCTCCGGTTGTATAAGATGAC
Ifitm1	GACAGCCACCACAATCAACAT	CCCAGGCAGCAGAAGTTCAT
Csf3r	CTGATCTTCTTGCTACTCCCCA	GGTGTAGTTCAAGTGAGGCAG
Slc7a11	AAGTCTAATGGGGTTGCCCT	TGATAGCCATGGAGATGCAG
Mmp8	TCAACCAGGCCAAGGTATTG	ATGAGCAGCCACGAGAAATAG
Mmp9	TTGGTTTCTGCCCTAGTGAGAGA	AAAGATGAACGGGAACACACAGG
Cxcl2	AAGTTTGCCTTGACCCTGAA	AGGCACATCAGGTACGATCC
Ccl6	ATGATGAGACATTCCAAGACTGC	TCAAGCAATGGCACTGTTCCCAGA
Hdc	GCGACCCTTCCTTCGAAATT	CCTTTAACACACTTTCTGTGAGACAAT
Cd33	CCGCTGTTCTTGCTGTGTG	AAGTGAGCTTAATGGAGGGGTA
Lilr4b	AGTGTCGTCACAAAAATAAGGCT	CCTGGGCGTACACAATTCCC
Mxd1	AGATGCCTTCAAACGGAGGAA	CAAGCTCAGAGTGGTGTGTCG
Il1b	ACAGCAATGATGAGGATCTGC	CTCTAGGTGGGTCTTGGGAAC